Advances in Water Resources 31 (2008) 915–925

Contents lists available at ScienceDirect

Advances in Water Resources

journal homepage: www.elsevier.com/locate/advwatres

Parameterization of the logarithmic layer of double-averaged streamwise velocity profiles in gravel-bed river flows

Mário J. Franca [a,*], Rui M.L. Ferreira [b], Ulrich Lemmin [c]

[a] Department of Civil Engineering and IMAR-CMA, University of Coimbra, Pólo II, 3030-788 Coimbra, Portugal
[b] Department of Civil Engineering and Architecture, Instituto Superior Técnico, TULisbon, Av. Rovisco Pais, 1049-001 Lisbon, Portugal
[c] Laboratoire d'Hydraulique Environnementale (LHE), École Polytechnique Fédérale de Lausanne, CH 1015 Lausanne, Switzerland

ARTICLE INFO

Article history:
Received 14 February 2007
Received in revised form 27 February 2008
Accepted 2 March 2008
Available online 18 March 2008

Keywords:
Double-averaged velocity profiles
Logarithmic law
Velocity field measurements

ABSTRACT

The logarithmic layer of double-averaged (in time and space) streamwise velocity profiles obtained from field measurements made in the Swiss rivers, Venoge and Chamberonne is parameterized and discussed. Velocity measurements were made using a 3D Acoustic Doppler Velocity Profiler. Both riverbeds are hydraulically rough, composed of coarse gravel, with relative submergences (h/D_{50}) of 5.25 and 5.96, respectively. From the observations, the flow may be divided into three different layers: a roughness layer near the bed, an equivalent logarithmic layer and a surface or outer layer. It was found that a logarithmic law can describe the double-averaged profiles in the layer $0.30 < z/h < 0.75$. The parameterization of the logarithmic law is discussed. Special emphasis is given to the geometric parameters roughness and zero-displacement heights and to the equivalent von Karman constant.

1. Introduction

A deep understanding of turbulent processes in open channels and rivers is needed in order to better formulate engineering solutions within such river disciplines as river restoration, pollution control and stable channel design. At present, laboratory experiments and numerical simulations are the main source of information for open-channel turbulence and for the interpretation of flow phenomena in rivers. These open-channel studies are typically carried out under idealized conditions of uniform flow and flat beds with a fairly homogeneous bed roughness distribution and are often designed to study specific aspects. Field studies in rivers are important in order to understand fluvial processes which cannot be reproduced in the laboratory. However, few field investigations in natural or canalized rivers have been made. Recent work on fluvial hydraulics, including field studies, was summarized by [11]. These authors classified the contributions by type of analysis and by topic (flow structure, velocity profiles, microhabitats and numerical model validation). Examples pertinent to the present research and not referred to by Buffin-Bélanger and Roy [11] include the following: Nelson et al. [31] described the turbulent structure in the wake formed by the presence of bed forms, which are responsible for the observed deviations in the lower layers of the velocity profile; Baiamonte et al. [4] showed the delay effect in the streamwise velocity produced by boulder drag in gravel-bed rivers; Smart [44] and Babaeyan-Koopaei et al. [3] studied time-averaged velocities, turbulence intensities, shear stresses, bed shear, friction velocity, roughness parameters and velocity spectra; Nikora and Smart [33] investigated the vertical distribution of turbulent energy dissipation and characteristic turbulence scales; Katul et al. [26] compared the velocity deviations produced in gravel-bed rivers with the inflected profiles observed in atmospheric flows above the vegetation canopy; Hurther et al. [23] documented the existence of coherent structures in rivers and their influence on transport and mixing; Tritico and Hotchkiss [46] described turbulence characteristics in the wake of obstructions. More references to field studies of fluvial hydraulics are given in [36] and in [15], thus extending the list by Buffin-Bélanger and Roy [11].

In river engineering, it is essential to estimate the vertical distribution of the streamwise flow velocity. For low relative submergence, i.e., for small values of h/D, where h is the water depth and D a geometry parameter representative of the bed roughness, generally a grain diameter, the streamwise velocity profile is not self-similar inside the roughness layer [33,44]. However, data obtained in gravel-bed flows with low relative submergence show that there exists a region above the roughness layer where a logarithmic distribution still adequately describes the vertical velocity distribution [8,14,44,18]. In this region, it is possible to parameterize the overall velocity distribution for gravel river flows with macro-scale roughness using an equivalent logarithmic 2D velocity profile [37,5]. Given the high spatial variability of the flow

* Corresponding author.
E-mail addresses: mfranca@dec.uc.pt (M.J. Franca), ruif@civil.ist.utl.pt (R.M.L. Ferreira), ulrich.lemmin@epfl.ch (U. Lemmin).

0309-1708/$ - see front matter © 2008 Elsevier Ltd. All rights reserved.
doi:10.1016/j.advwatres.2008.03.001

characteristics in gravel-bed rivers with low relative submergence, the application of double-averaged (in time and space) methods (DAM) seems appropriate, providing flow characteristics are averaged over at least one wavelength of the bed-form [45,40]. In hydraulics, the DAM approach was adopted by the authors in [34,28,1,39,38], amongst others.

This paper aims at (i) proposing a division of the identified flow regions of gravel-bed rivers with low submergence and, accordingly, (ii) to parameterize the distribution of the streamwise velocity over the flow depth.

Empirical results are presented from two field measurement campaigns made in the Swiss gravel-bed rivers, Venoge and Chamberonne. Using the D_{50} of the bed surface as the geometry parameter representative of the bed roughness, the relative submergence for the two rivers is 5.25 and 5.96, respectively. Dittrich and Koll [14] classified rivers as shallow, i.e., with low relative submergence, when the ratio h/D is lower than 5. By this definition the present measurements can be considered at the limit of low relative submergence. Profiles of the streamwise velocity are studied. A logarithmic equation is found suitable to describe the observed profiles in an equivalent logarithmic region in the intermediate layer of the flow and its parameters are quantified from the presented field data. This parameterization is compared with current theories for the description of the streamwise velocity distribution in rough turbulent river flows with irregular boundaries and low relative submergence.

In the next section, an introduction to the theory of double-averaging methods and velocity profile parameterization in the logarithmic layer is given. Field measurement conditions and the instrumentation (ADVP – Acoustic Doppler Velocity Profiler) are then presented, followed by the empirical results and the conclusions.

2. Theoretical background

2.1. Double-averaged velocity profile

For 3D, isothermal, turbulent open-channel flows of incompressible Newtonian fluids, continuity and conservation of mean momentum may be expressed using the Cartesian tensor notation (see [22]), respectively,

$$\frac{\partial \overline{u_j}}{\partial x_j} = 0, \tag{1}$$

$$\rho \frac{\partial \overline{u_i}}{\partial t} + \rho \overline{u_j} \frac{\partial \overline{u_i}}{\partial x_j} = \rho \overline{f_i} - \frac{\partial \overline{P}}{\partial x_i} + \frac{\partial}{\partial x_j}\left(\tau_{ij}^{(v)} + \tau_{ij}^{(t)}\right). \tag{2}$$

Eq. (2) is the Reynolds Averaged Navier–Stokes equation (RANS). In this equation, t stands for the time variable, x for the space variable, u for velocity, subscript i and j for the 3D Cartesian directions with 1 for streamwise, 2 for spanwise and 3 for vertical, P for pressure, ρ for density, f for the mass forces (for open-channel flows as the ones herein analyzed these correspond to the gravity term: $f_i = g\delta_{i3}$, where δ is the Kronecker symbol), $\tau^{(v)}$ for mean viscous stresses $\left(\tau_{ij}^{(v)} = \rho\nu\left(\frac{\partial \overline{u_i}}{\partial x_j} + \frac{\partial \overline{u_j}}{\partial x_i}\right)\right.$, where ν is the kinematic viscosity), and $\tau^{(t)}$ for turbulent or Reynolds stresses $(\tau_{ij}^{(t)} = -\rho\overline{u_i' u_j'})$. The over-bar indicates time-averaging and the prime stands for instantaneous fluctuations. The streamwise, spanwise and vertical directions are identified by x, y and z, and the corresponding velocities, by u, v and w.

The terms of the left-hand side of Eq. (2) represent the mean momentum variation due to unsteadiness and convection; assuming steady flow conditions, the term representing unsteadiness ($\partial/\partial t$) may be eliminated.

For practical applications, i.e., the estimate of flow resistance, precise 3D details of river flows are not essential and often a 2D description of the velocity distribution is sufficient. 2D vertical velocity profiles should correspond to real 3D velocity distributions in terms of local averaged momentum. The RANS equations are not suitable for flows over irregular rough boundaries especially in the near-bed region where the flow is highly 3D and heterogeneous. In order to incorporate the effect of boundary local topography, a spatial averaging operation may be applied to the RANS equations, resulting in the so called double-averaged (in time and space) Navier–Stokes (DANS) equations. Double-averaged velocity (in time and space) as defined by [34] becomes

$$\langle \bar{u} \rangle(z) = \frac{1}{A(z)} \int_{\Omega(\alpha,\beta)} \bar{u}(\alpha,\beta,z)\mathrm{d}S, \tag{3}$$

where Ω is, without loss of generality, a rectangular domain whose area is $L_x \times L_y$, located parallel to the plane z = const (assumed parallel to the bed). Both L_x and L_y should be large when compared with the wavelengths of the spatial distributions of the variations of the near-bed longitudinal velocities (cf. [45]). The area, within Ω, occupied by fluid at a given elevation, is A. Function $A(z)$ expresses the void distribution between the lowest troughs and the highest crests of the roughness elements. Dummy variables α and β are such that $0 < \alpha < L_x$ and $0 < \beta < L_y$. Evidently, the time-averaged velocity $\bar{u}$ is defined only in the points $\alpha, \beta \in \Omega$ occupied by fluid. The integration is made over a horizontal surface ($\mathrm{d}S$). It is assumed that the distribution of the roughness elements is isotropic and homogeneous; hence, line-averaging along a perpendicular to the riverbank becomes equivalent to area averaging. From spatially discrete measurements of velocity profiles, the calculation of the double-averaged velocity is defined by

$$\langle \bar{u} \rangle(z) = \frac{\sum_{k=1}^{N-N_0(z)} \bar{u}_k(z) A_k(z)}{\sum_{k=1}^{N-N_0(z)} A_k(z)} \cong \frac{1}{N - N_0(z)} \sum_{k=1}^{N-N_0(z)} \bar{u}_k(z), \tag{4}$$

where $A_k(z)$ is the area occupied by fluid of a convex sub-domain Ω_k, defined as the area of influence of $(x_k,y_k) \in]0,L_x[\times]0,L_y]$ and such that $\bigcup_{k=1}^{N(z)} \Omega_k = \Omega$, N represents the total number of sub-domains and $N_0(z)$ the number of sub-domains, at elevation z, for wich the velocity is not defined at (x_k,y_k). It should be noted that, in general, $\sum_{k=1}^{N-N_0(z)} A_k(z) \leqslant A(z)$. The simplified expression obtained on the right hand side is only appropriate for measurements with a regular grid spacing. Similar to the concept of Reynolds decomposition, the time-averaged terms may be decomposed into a space average (double-averaged) and a mean spatial deviation

$$\begin{aligned} \bar{u}(x,y,z) &= \langle \bar{u} \rangle(z) + \tilde{u}(x,y,z); \langle \tilde{u} \rangle = 0, \\ \bar{P}(x,y,z) &= \langle \bar{P} \rangle(z) + \tilde{P}(x,y,z); \langle \tilde{P} \rangle = 0, \end{aligned} \tag{5}$$

where the tilde denotes the difference between the double-averaged and time-averaged values and the square brackets denote spatial averaging. Double-averaged variables are the same for all points within the averaging domain.

2.2. Logarithmic law

Three different length scaling parameters exist for the description of a turbulent boundary layer flow: two inner scales, the viscous length ν/u^*, where u^* is the bed friction velocity and the roughness length k_s; and an outer scale defined typically by the boundary layer thickness or, as in the present case, by the flow depth, h. Using dimensional analysis, the velocity gradient may be expressed as a function of these geometric and velocity scales. At high relative submersions and at sufficiently high Reynolds numbers, and regardless of the nature of the boundary, an overlap region exists where complete similarity may be assumed [6], thus making the derivation of a logarithmic law for the velocity distribution possible:

$$\frac{\langle\bar{u}\rangle(z)}{u*} = cte\ln z + A, \tag{6}$$

where *cte* and A are constants of integration. For the determination of the logarithmic law it is assumed that u^* is the velocity scale responsible for the momentum transfer from the outer to the inner layer and thus is valid for both flow regions ([38]). This overlap region is considered to be sufficiently far from both boundaries, $zu^*/\nu \gg 1$ or $z/k_s \gg 1$ and $z/h \ll 1$, thus making the distance z the remaining relevant length scale. The existence of a logarithmic layer implies a clear separation between the inner and outer regions. For low submergence flows, this may not occur and thus no overlap region may actually exist.

For the definition of the logarithmic layer of the velocity profile, the level of the lower integration boundary is important. For hydraulically turbulent rough flows, Nikuradse defined the equivalent roughness height k_s as the lower integration boundary [30]. However, for macro-scale roughness with irregular distribution, k_s is no longer suitable as an integration boundary. [13] introduced zero-plane displacement height (d) as the origin of the logarithmic profile. [35] redefined the concept of zero-plane displacement height by stating that this represents the position where large-scale eddies "feel" the river bed. According to this definition, the zero-plane displacement height corresponds to a level where Prandtl's mixing length is zero. This is equivalent to the level where the vertical gradient of the streamwise velocity tends to infinity. Herein, we will consider the following logarithmic parameterization of the logarithmic profile [35],

$$\frac{\langle\bar{u}\rangle(z)}{u_e*} = \frac{1}{\kappa_e}\ln\left(\frac{z-d}{z_R-d}\right) + \frac{\langle\overline{u_R}\rangle}{u_e*} \tag{7}$$

where u_e^* is the equivalent friction velocity for the double-averaged velocity profile, z_R the lower limit of the layer where the logarithmic law is valid, also known as the roughness height, and $\langle\overline{u_R}\rangle$ is the double-averaged velocity at the integration level $z = z_R$. In other words, $\langle\overline{u_R}\rangle$ is the slip velocity at the level z_R imposed as a lower boundary condition. The plane defined by $z = d$ is situated somewhere between the top of the roughness layer and the roughness troughs. The parameter κ_e is an integration constant analogous to the von Karman constant (hereinafter it will be called the equivalent von Karman constant). The von Karman constant (κ) was empirically determined for flows where complete similarity exists in the overlap region. It was therefore considered to have a universal value, commonly assumed to be $\kappa \approx 0.41$. If the overlap region does not exist, as in the case of low relative submergence flows, the value of κ_e may be different from that of κ and a function of the bed roughness. For practical purposes, the equivalent friction velocity may be estimated from variables easily measurable in the field with the uniform flow based expression

$$u_e^* = \sqrt{g(z_w - \overline{z_0})S}, \tag{8}$$

where z_w is the water elevation, $\overline{z_0}$ the mean bed elevation, and S is the streamwise river bed slope. Several authors showed that the maximum shear stress appears at an elevation close to the roughness element crests [32,2,17]). It is implicit in expression (8) that the origin of a hypothetical linear shear stress distribution is $\overline{z_0}$.

3. Field study

Field measurements of velocity profiles were carried out during the summer of 2003, in the rivers Venoge and Chamberonne. Both are lowland rivers (Fig. 1) and are located in the canton of Vaud, Switzerland. Investigations were made across one section on a straight river (Fig. 2) reach during summer periods (low water). On both cases, due to the difficulty on assuring a position of the traversing system perpendicular to the river bank, we corrected the angle of the measurements with an algorithm that allowed the minimal spanwise component of the velocity in average for all the profiles. This way, and for the Chamberonne case, a spanwise component fairly constant across the section and caused by the presence of a smooth bend located upstream of the gauging section, was reduced to negligible values. The cross sections are located at the following sites: in the river Venoge, 120 m upstream from the Moulin de Lussery and in the river Chamberonne, 385 m upstream from the river mouth (Fig. 2). Table 1 summarizes the flow conditions.

In Table 1, Q is the flow discharge, h the mean water depth, B the river width, Re the Reynolds number ($Re = Uh/\nu$, where U is the cross-section averaged streamwise velocity ($U = Q/(Bh)$) and ν the kinematic viscosity taken as $1.01 \times 10^{-6}\ m^2\ s^{-1}$), Fr the Froude number ($Fr = U/\sqrt{gh}$, where g is the acceleration of gravity) and D_{50} the width of the square mesh of the sieve that retains 50%, in weight, of the bed material samples.

Based on the average water depth, the ratio B/h is 30 and 20 for the rivers Venoge and Chamberonne, respectively. Both rivers therefore correspond to wide channels. The streamwise river bed slope was determined locally with topographic data obtained from [25] for the Venoge and for the Chamberonne from the Gesrau system (SESA – Canton of Vaud). At the time of the measurements, both river bottoms had a gravel-armoured layer.

For each river, all measurements were taken on a single day. The discharge in the river sections was constant during the measurement time, as was confirmed by discharge data provided by

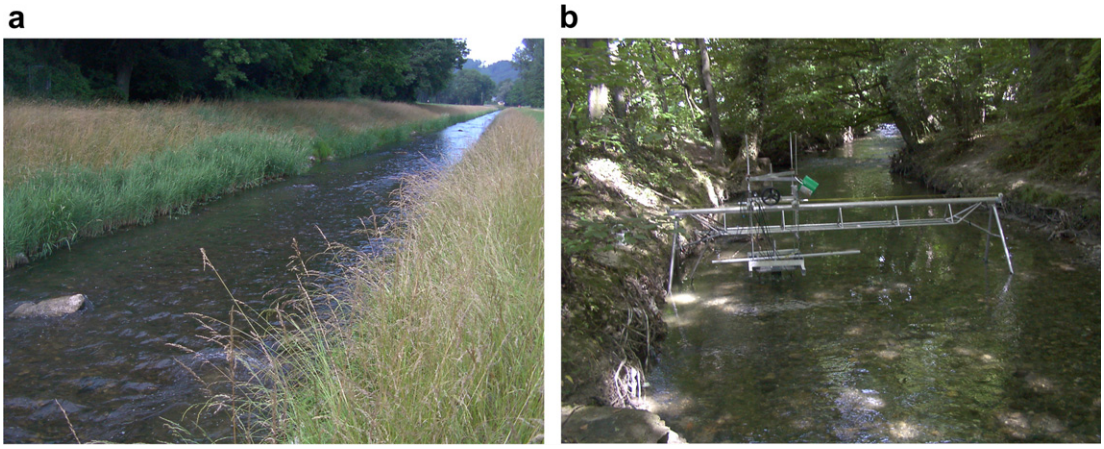

Fig. 1. View of the study reaches of the rivers (a) Venoge and (b) Chamberonne.

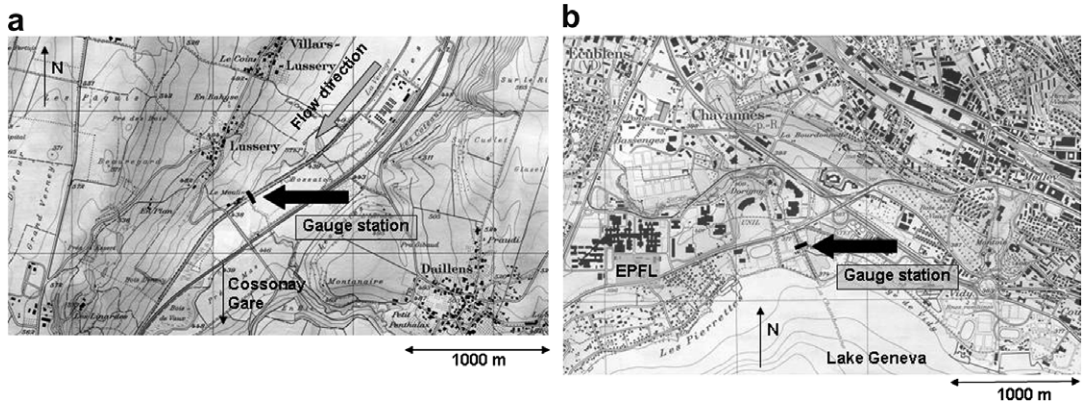

Fig. 2. (a) Location of the gauge station in the river Venoge (extract from topographic map Nr. 1222, reproduced by permission of swisstopo (BA081185), Switzerland); (b) Location of the gauge station in the river Chamberonne (extract from topographic map No. 1243, reproduced by permission of swisstopo (BA081185), Switzerland).

Table 1
Summary of the flows and of the boundary characteristics

River	S (%)	Q (m^3/s)	h (m)	B (m)	Re ($\times 10^4$)	Fr	u_e^* (m/s)	D_{50} (mm)	h/D_{50}
Venoge	0.33	0.80	0.21	6.30	12.6	0.42	0.078	40	5.25
Chamberonne	0.26	0.55	0.29	5.75	9.5	0.19	0.085	49	5.96

the Swiss Hydrological and Geological Services. Hydraulic conditions in the rivers are thus considered constant. Measurements were made only in one-half of the cross section of the rivers, starting from the right riverbank in both cases. For the river Venoge, 25 profiles were measured, each over a 5 min period, with a horizontal spacing of 10–12.5 cm. For the river Chamberonne, 24 profiles were measured, also during 5 min each, with a horizontal spacing of 5–12.5 cm. It was verified that a 5-min recording period was a sufficiently long time to represent the first and second order moments of the instantaneous velocity signals. The vertical resolution of the measurements was about 0.5 cm. The sampling grid covered areas perpendicular to the streamwise direction, corresponding to 0.60 and 0.73 m^2, with sampling densities of 884 and 693 points/m^2, for the Venoge and Chamberonne, respectively. During the measurements, no sediment transport occurred.

4. Instrumentation

The measurements were made with the 3D ADVPs developed at the Laboratoire d'Hydraulique Environnementale, École Polytechnique Fédérale de Lausanne (LHE). It is a non-intrusive ultrasonic instrument capable of measuring quasi-instantaneous 3D velocity profiles of clear water flows over the entire flow depth. The ADVP does not disturb the flow since ultrasound receivers are in a separate box located at the top of the water column (cf. [19]). It may be used for laboratory and field studies (rivers and lakes). Details on the working principle of this Doppler based instrument are given in [41]. In Doppler-based velocimeters, the signal emitted by the ultrasonic emitter-transducer is backscattered by moving targets and captured by receiver-transducers. The Doppler frequency shift observed between the emitted and the received signal is proportional to the target's velocity in the receiver direction. The quality of the signal depends on the scattering targets and their ability to follow the fluid motion [43]. The ADVP is a flexible instrument, since the instrument and the acquisition parameters can be permanently adjusted to the conditions during the measurements. The data quality

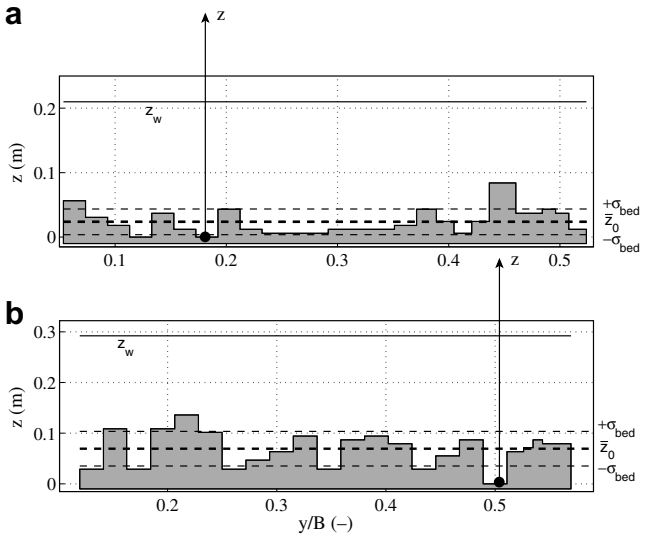

Fig. 3. River bed profiles across the section of the rivers (a) Venoge and (b) Chamberonne.

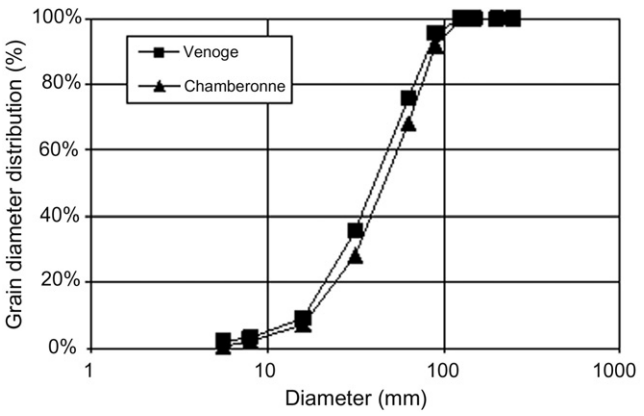

Fig. 4. Bed grain diameter distribution for both rivers (grain samples were taken from the armoured layer).

is controlled by oscilloscope before and during recording, thus allowing to assure an optimal configuration of the system. The ADVP configuration used for the present measurements consists of four receivers that surround the emitter. This provides one redundancy in the 3D velocity component calculation which is used to eliminate signal noise and to control the data quality [24,9].

For both rivers, a pulse repetition frequency (PRF) of 2000 Hz and a number of pulse pairs (NPP) equal to 32 was used, which results in a sampling frequency of 62.5 Hz. Although a low degree of aliasing was expected, a dealiasing algorithm developed by [19] was applied to the data. This correction, combine with the use of a multistatic configuration, allows theoretically noise-free 3D velocity estimations (cf. [19,9]). For the transversal displacement of the ADVP system, a portable metal bridge structure (Fig. 1b) was installed and leveled so that the instrument was always at the same distance from the water surface. This set-up allowed efficient profiling and minimum disturbance of the flow by the measuring installation and at the same time minimized the flow-induced vibration of the ADVP.

5. Results

5.1. River bed

The local river bed level is determined from the acoustic backscatter response. For each profile, the position of the bottom is detected by a saturation of the ADVP signal in the region corresponding to the riverbed, allowing to determine it with a precision of about 5 mm. Fig. 3 shows the bed level variation across the river sections.

The origin of the vertical coordinates was chosen to be the lowest measured point (designated as bed origin of type 3(1) by [35];

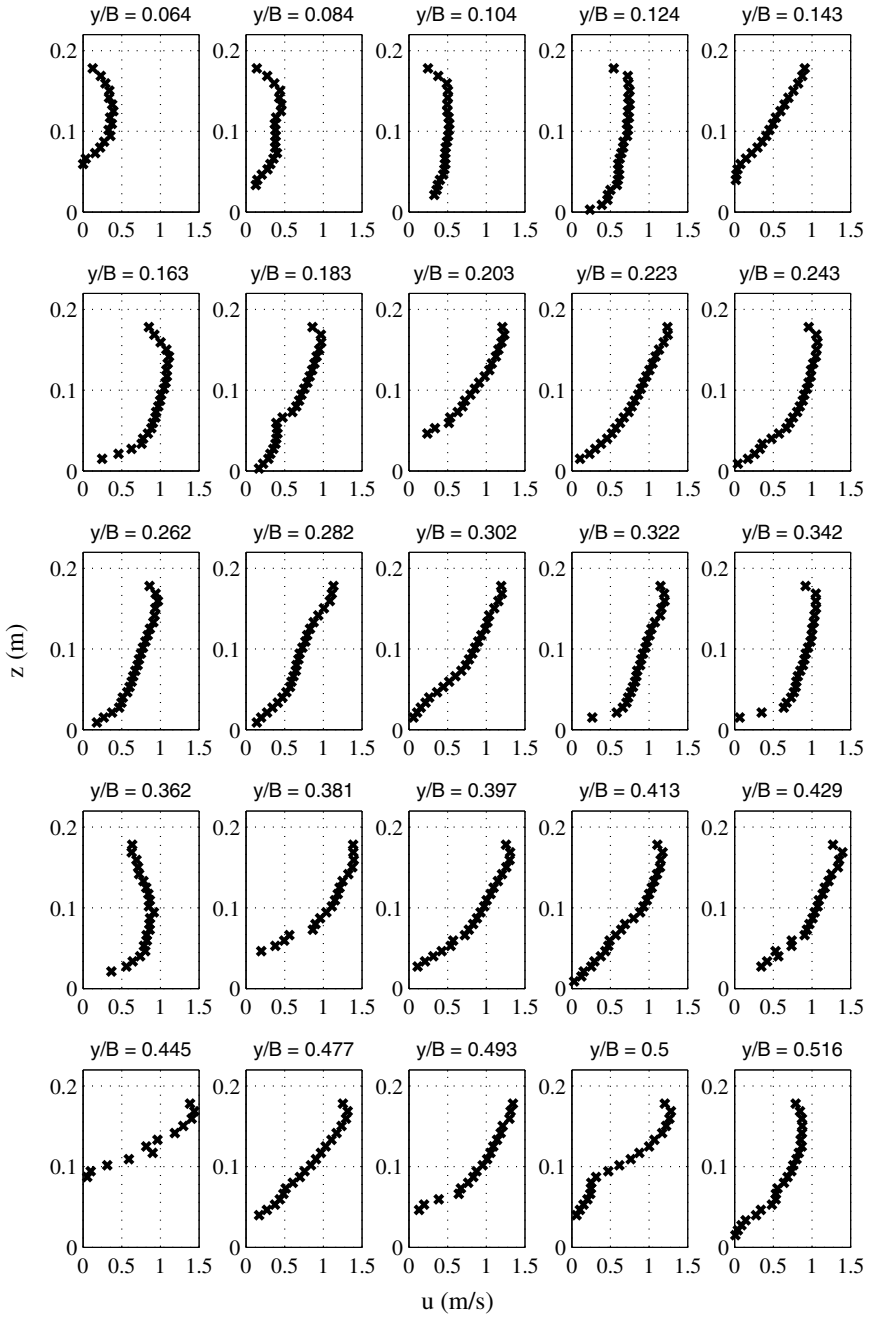

Fig. 5. Measured time-averaged velocity profiles for the river Venoge.

Fig. 3). The mean bed elevations are $\overline{z_0} = 0.024$ and 0.069 m ($\overline{z_0} = 0.11h$ and $0.24h$), and the standard deviations of the bed elevations are $\sigma_{bed} = 0.020$ and 0.033 m; for the rivers, Venoge and Chamberonne. [27] characterized the roughness irregularity of the bed by the parameter σ_{bed}/D. In the present cases, taking $D = D_{50}$ we find $\sigma_{bed}/D_{50} = 0.50$ and 0.66 for the Venoge and the Chamberonne, respectively.

For both rivers, bed sediments were sampled and analyzed according to the sample collection method for coarse rivers proposed by Wolman [47]. The bed material samples were taken from the armoured layer and, in both cases, more than 100 gravel stones were collected.

Standard sieve sizes were used to obtain the grain size distribution of the riverbed material as shown in Fig. 4. As indicated in Table 1, the bed surfaces of the rivers Venoge and Chamberonne have median grain diameters of 40 and 49 mm, respectively. By definition, both riverbeds are composed of coarse gravel.

5.2. Time-averaged velocity profiles

Figs. 5 and 6 show the different measured velocity profiles, time-averaged over the entire measuring period for both rivers. The profiles are all referenced to the lowest bed elevation in the measured river section, which results in water depths $h = 0.210$ and 0.292 m for the Venoge and Chamberonne, respectively. Lateral distances indicated are normalized by the river width with the origin on the right riverbanks.

Deviations from a logarithmic velocity profile are visible in the upper layers of the flow, especially for the Chamberonne river. It is difficult to establish a general tendency in the observed deviations,

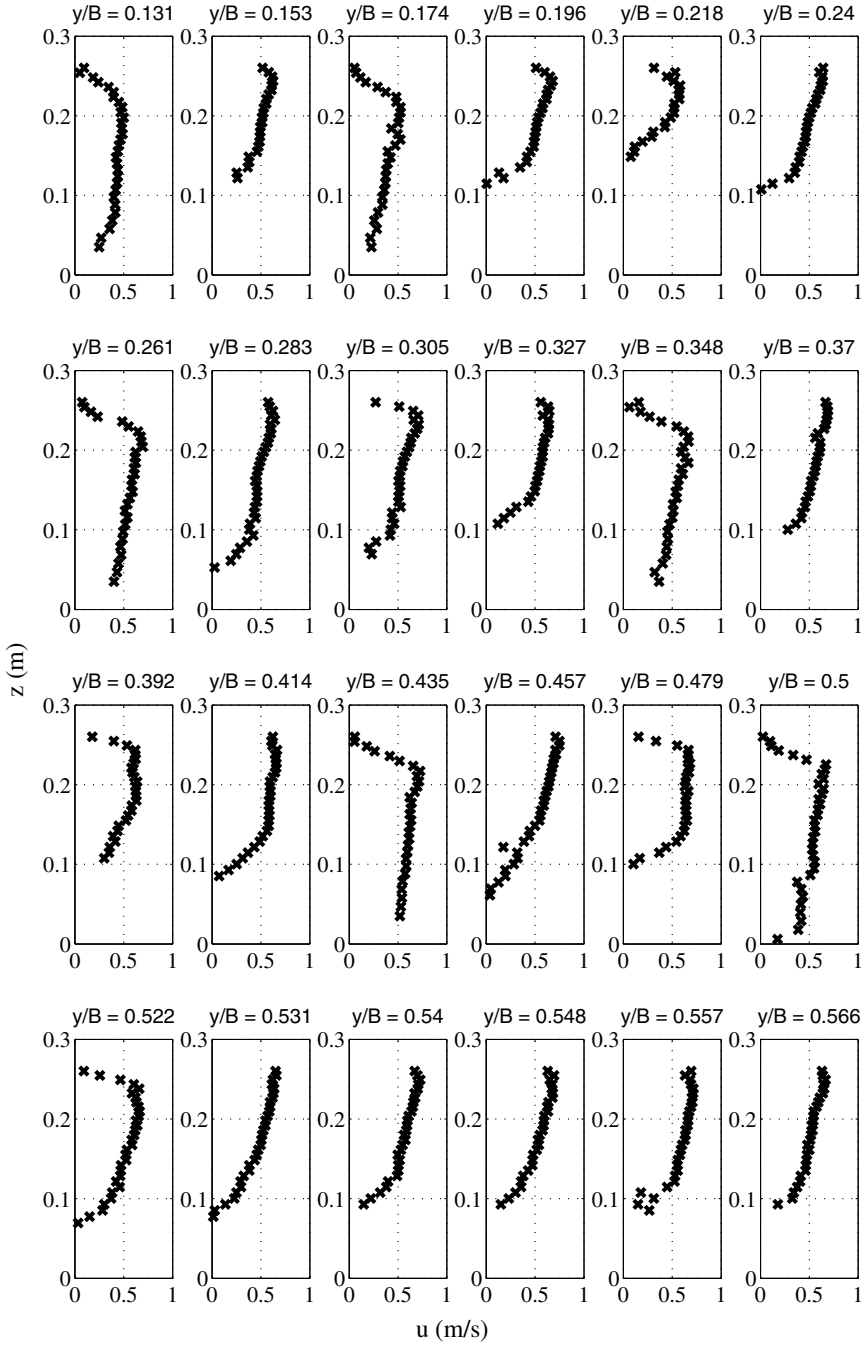

Fig. 6. Measured time-averaged velocity profiles for the river Chamberonne.

because they occur in both upstream and downstream directions by a relative increase or decrease of the flow velocity. In decelerating flows, the time-averaged velocity profile in gravel-bed rivers may acquire a so-called D-shape ([16]).

In some velocity profiles, a wake effect near the bed is observed, which may be caused by a sudden change of the bed level or roughness upstream from the measuring point, as observed by Carravetta et al. [12]. This feature is most evident in profiles corresponding to $y/B = 0.183$, 0.282, 0.445, 0.500 and 0.516 in the Venoge. Such velocity deviations in the lower layers of the flow are widely observed in gravel-bed rivers in the presence of large bed protuberances [29,7,10,21].

From the analysis of the time-averaged velocity distribution throughout the corresponding cross-section measurements, [18,20] noticed that an influence of the riverbank on the time-averaged streamwise velocity distribution exists for $y/B < 0.15$. Thus, the side wall effect disappears for $y/h > 4.5$ and 3.0, for the Venoge and Chamberonne, respectively. Fig. 7 shows the lateral variation of the time-averaged velocities measured at $z/h = 0.50$. No significant lateral variation is observed in the time-averaged velocity,

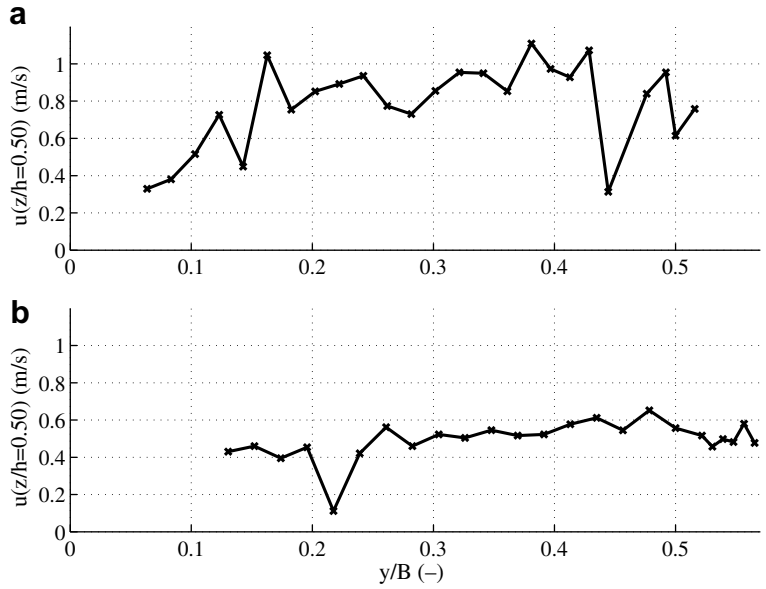

Fig. 7. Time averaged streamwise velocities measured at $z/h = 0.50$ (a) Venoge and (b) Chamberonne.

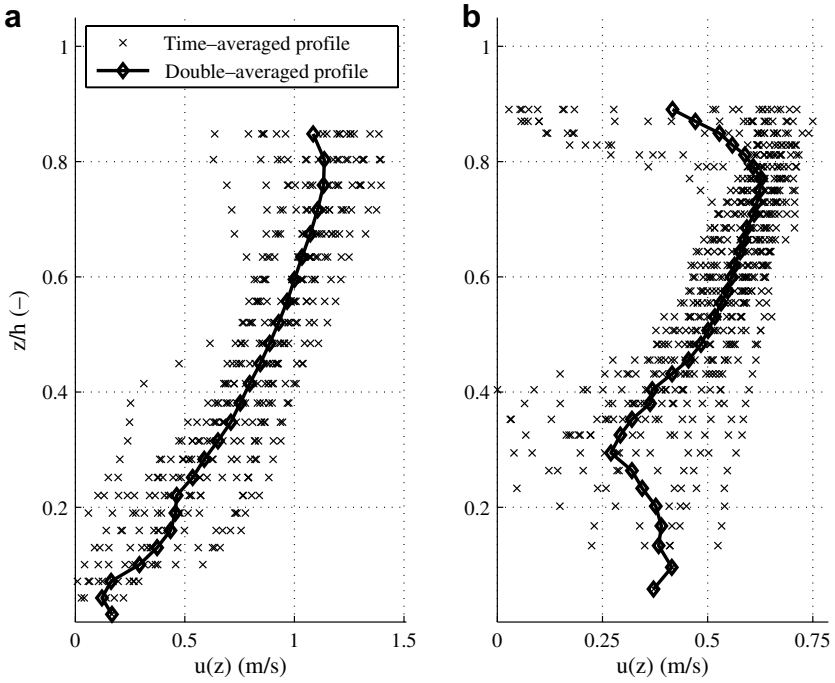

Fig. 8. Time- and double-averaged (thick lines) velocity profiles for the rivers (a) Venoge and (b) Chamberonne.

because the velocity tends to a fairly constant value in both cases within the central region of the flow.

5.3. Double-averaged velocity profiles

For the calculation of the equivalent double-averaged streamwise velocity profile, the measurements taken at $y/B < 0.15$ will not be considered. Spurious profiles from two measurements (located at $y/B = 0.445$ for the Venoge and at $y/B = 0.218$ for the Chamberonne) are not considered in the subsequent analysis either. Fig. 8 shows the time-averaged and the double-averaged velocity profiles for both rivers.

From the analysis of the double-averaged velocity profiles, it is evident that the flow may be divided into the following three layers: inner, intermediate and outer. Furthermore, a well defined logarithmic layer can be identified within the intermediate region of the flow, extending roughly from $z/h \approx 0.20$–0.80. In the next section, we will apply a procedure to define the limits of this intermediate flow region and parameterise the log-laws that best-fit the empirical double-averaged velocity distributions for both rivers.

5.4. Equivalent Von Karman constant (κ_e) and zero-plane displacement height (d)

In order to use the definition of zero-plane displacement height as suggested by Nikora et al. [35], we assume that an analogous Prandtl's mixing length concept [30] is valid for the double-averaged velocity profiles within the intermediate layer. Thus, we may relate the total shear stress to the gradient of the double-averaged velocity as follows:

$$\tau = \rho u_{e*} l_e \frac{\partial \langle \bar{u} \rangle}{\partial z}, \tag{9}$$

where l_e is the equivalent mixing length. The derivation of the logarithmic law for the description of the streamwise velocity by the momentum flux approach implies that the shear stress is constant within the logarithmic layer. Thus, from the definition of friction velocity $u_{e*}^* = (\tau/\rho)^{0.5}$, one obtains

$$l_e = u_{e*} \left(\frac{\partial \langle \bar{u} \rangle}{\partial z} \right)^{-1} \tag{10}$$

According to Nikora et al. [35], the zero-plane displacement height corresponds to the position in the water column where the mixing length is zero, i.e., $l_e(z = d) = 0$. Equating (7) and (10), the following relationship between the mixing length (l_e) and the equivalent von Karman constant may be established:

$$l_e = u_{e*} \left(\frac{\partial \langle \bar{u} \rangle}{\partial z} \right)^{-1} = \kappa_e (z - d) \tag{11}$$

The equivalent von Karman constant may thus be determined by the slope of a linear regression of l_e against $(z - d)$.

Rearranging Eq. (7), the equivalent von Karman constant may also be estimated from the following linear relationship:

$$\kappa_e \underbrace{\frac{\langle \bar{u} \rangle (z) - \langle \overline{u_R} \rangle}{u_{e*}}}_{I} = \underbrace{\ln \left(\frac{z - d}{z_R - d} \right)}_{II}. \tag{12}$$

With all terms of Eq. (12) empirically established, κ_e can be estimated for several positions within the logarithmic layer of the double-averaged velocity profiles. We will use Eq. (12) to establish the limits of the logarithmic layer and Eq. (11) to parameterize κ_e and d.

The plot of the quotient of term II by term I on Eq. (12) allows us to infer the subregion of the flow where the equivalent von Karman constant remains invariable; based on this plot we may thus define limits of the intermediate flow region where a logarithmic parameterization of the double-averaged velocity profile is valid (z_R and z_L). Within these limits we may now calculate d and κ_e using a linear regression between l_e versus z (see Eq. (11)). With d estimated from the latter linear regression we may look back to Eq. (12) and validate the boundaries z_R and z_L previously found or re-establish new ones. A trial and error procedure is thus delineated where convergence to a definition of the logarithmic subregion based on Eq. (12) and to the establishment of d and κ_e parameters is expected.

As a first approach, based on the observation of Fig. 8, we set up the following parameters: $d = \overline{z_0} = 0.021$ and 0.068 m; $z_R = 0.046$ and 0.086 m; $\langle \overline{u_R} \rangle = 0.463$ and 0.270 m/s, for the Venoge and Chamberonne, respectively. After the application of the referred trial and error procedure, the best solution obtained with the present data corresponds to Figs. 9 and 10.

In Fig. 9, where equivalent Von Karman calculation is made with Eq. (12), one may identify subregions of the flow where κ_e converges to constant values ($\kappa_e \approx 0.19$ and 0.33 for the Venoge and Chamberonne), thus where the logarithmic law defined by Eq. (7) is valid. This region is situated between $z_R \approx 0.30\ h$ and $z_L \approx 0.75h$. The roughness height (z_R) scales with $1.7D_{50}$ and with $2.1D_{50}$ for the Venoge and the Chamberonne cases. The double-averaged velocities at $z = z_R$ are $\langle \overline{u_R} \rangle = 0.65$ and 0.32 m/s and, at $z = z_L$, they are $\langle \overline{u_L} \rangle = 1.13$ and 0.62 m/s, for the Venoge and the Chamberonne, respectively. The upper limit of the logarithmic layer is approximately $4.0D_{50}$ for both cases.

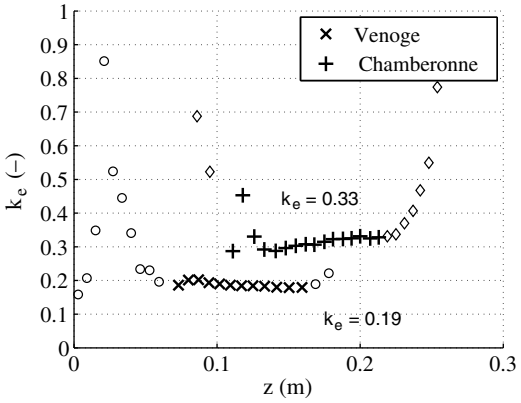

Fig. 9. Determination of the equivalent von Karman constant κ_e (using Eq. (12)). Circles and diamonds correspond to points outside the logarithmic layer for the Venoge and Chamberonne, respectively.

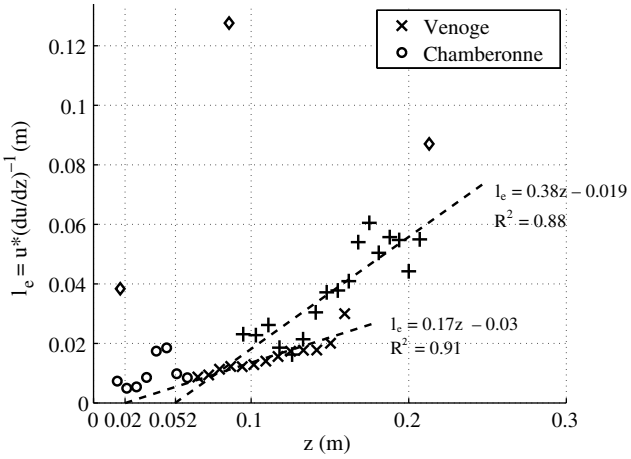

Fig. 10. Determination of the zero-plane displacement height d and von Karman constant κ_e (using Eq. (11)). Circles and diamonds correspond to points outside the logarithmic layer for the Venoge and Chamberonne, respectively.

Fig. 10 shows the values of l_e and κ_e calculated from Eq. (10), inside the layer $z_R < z < z_L$, for both rivers. The velocity gradient of the double-averaged velocity profiles was calculated from a two-point running mean in the vertical. A linear regression with high correlation coefficients was found for both data sets. The values of d correspond to the points where the regression line intercepts the horizontal axis. Spurious points other than those shown in the figure were not considered for the estimate of d.

Despite the low relative submergence, the values of the mixing length follow fairly well a linear trend in both cases. The assumptions of constant shear stress and of linearity of the mixing length appear to be adequate for a wide region of the flow depth. The values of zero-plane displacement height are $d = 0.020$ and 0.052 m, and of equivalent Von Karman constant $\kappa_e = 0.17$ and 0.38, for the Venoge and Chamberonne cases, respectively. The zero-plane displacement heights are between 0.30 and 0.50 times the roughness height (z_R), and 0.50 and 1.06 times D_{50}, respectively for the Venoge and Chamberonne rivers. The values of d roughly scale with 0.80 times the mean bed elevations; we found $d = 0.83\overline{z_0}$ and $d = 0.75\overline{z_0}$, for the Venoge and Chamberonne, respectively. We consider the latter κ_e values for the parameterization of the log-profile since their determination is less dependent on z_L and z_R.

For the river Chamberonne, the value of κ_e is close to that of the von Karman constant which is valid for flows with a clear overlap region and consequently complete similarity. For the Venoge river, a constant κ_e value confirms the existence of a log adaptable region of the flow.

5.5. Parameterization of the logarithmic layer of the double-averaged velocity profile

The parameters of the theoretical logarithmic law (Eq. (7)) adjustable to the double-averaged velocity profiles, and obtained from the procedure described in the previous subsection of the text, are given in Table 2. Fig. 11 presents the double-averaged profiles obtained from the measurements and the parameterized velocity profile defined by Eq. (7). Good correlation factors between the double-averaged velocity profiles and the parameterized logarithmic law, calculated within the logarithmic layer, are found: $R^2 = 0.999$ for the Venoge; and $R^2 = 0.995$ for the Chamberonne.

In both rivers, three distinct flow regions are well defined: the roughness layer, situated below z_R (the roughness height, z_R, is situated above the mean level of the roughness crests, $\overline{z_0} = 0.11h$ and $0.24h$, respectively); a logarithmic layer between z_R and z_L; and an outer layer also called surface influenced layer situated above z_L.

Inside the roughness layer, random deviations of the velocity profile occur, especially for the Chamberonne river, indicating that the flow structure is 3D and totally conditioned by the bed roughness. For $z < z_R$, in the Venoge river, a distribution similar to an internal logarithmic boundary layer may be suggested, as was described by Sanford and Lien [42] and Franca [21]. In the Chamberonne case though, no coherent distribution of the time-averaged velocity is evident below z_R. In low relative submergence cases with randomly distributed bed protuberances, self-similarity of the flow does not exist inside the roughness layer [33,44]. In the

Table 2
Parameters for the logarithmic layer of double-averaged velocity profiles

River	z_L (m)	z_L/h	z_R (m)	z_R/h	d (m)	d/h	u_e^* (m/s)	u_R (m/s)	u_R/u_e^*	κ_e
Venoge	0.159	0.76	0.066	0.31	0.020	0.10	0.078	0.651	8.35	0.17
Chamberonne	0.213	0.73	0.103	0.35	0.052	0.18	0.085	0.320	3.76	0.38

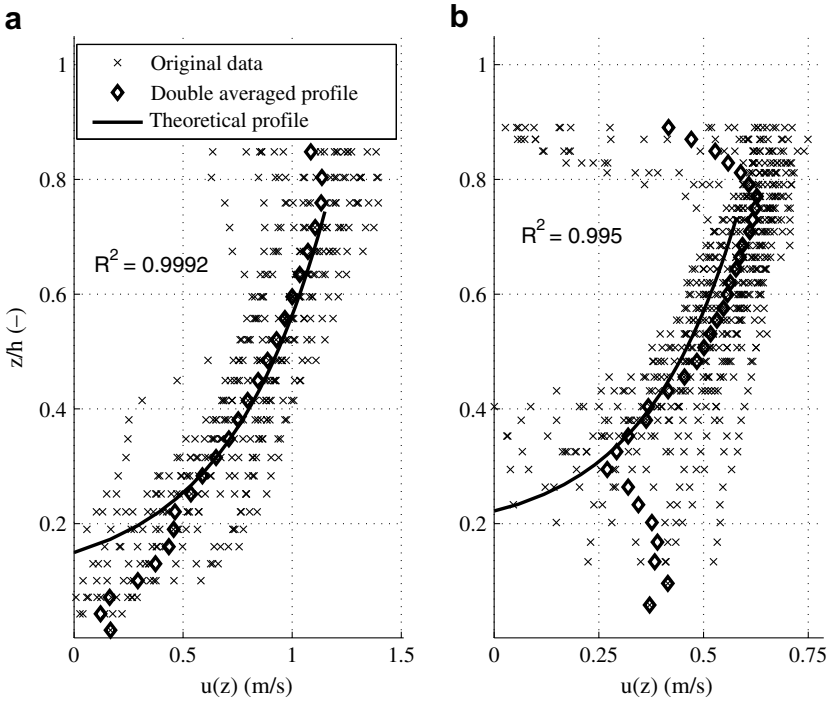

Fig. 11. Time-averaged, double-averaged and theoretical logarithmic velocity profiles for the rivers (a) Venoge and (b) Chamberonne.

intermediate layer the double-averaged profiles from the empirical data are well described by a logarithmic fit (Fig. 11), despite the low relative submergence of the flow.

It can be seen in Figs. 5, 6 and 8 that some velocity profiles have strong deviations from the logarithmic shape in the outer layer, most likely due to permanent 3D structures in the flow [16,5,48,20]). Franca [20] showed the occurrence of organized time-averaged secondary motion in these flows which is confined to the outer layer ($z > \approx 0.80h$). The limit of the surface layer (z_L/h) is still under discussion, and is usually attributed a lower value of z_L/h. The low relative submergence may induce a general wake effect shifting the logarithmic layer to a higher level.

6. Conclusions

In this paper, field measurements of streamwise velocity profiles taken in the rivers Venoge and Chamberonne with a deployable ADVP were analyzed. The river beds were composed of coarse gravel and the relative submergences were $h/D_{50} = 5.25$ and 5.96. Both rivers had a bed roughness irregularity parameter of $\sigma_{bed}/D_{50} \approx 0.50$ and 0.66. It was shown that, despite the low ratio h/D_{50}, there exists a region in the velocity profiles where the velocity distribution may be described by a logarithmic law. According to the present results, the flow can be divided into three different layers: a roughness layer, a logarithmic layer (determined by a best fit approach) and a surface or outer layer. Double-averaged velocity profiles were parameterized in the logarithmic layer, using the definition of the zero-plane displacement proposed by Nikora et al. [35].

The lower limit of the logarithmic layer is situated at $z_R/h \approx 0.30$, scaling with $\approx 2D_{50}$. Below the roughness height, two different situations can be observed. In the Venoge river, an organized structure of an internal logarithmic boundary layer seems to exist, whereas in the Chamberonne river the velocity distribution does not show a consistent pattern.

The upper limit of the logarithmic layer corresponded in both cases to $z_L/h \approx 0.75$, or $z_L \approx 4.0D_{50}$. There is still some uncertainty as to the level of the lower limit of the surface layer (z_L/h). Usually, a lower value than the one which we observed is attributed to z_L/h. The low relative submergence possibly induces a general wake effect which shifts the logarithmic layer to a higher level.

Estimating empirically the equivalent von Karman constant and the zero-displacement height, we obtain values of $\kappa_e = 0.17$ and 0.38, and of $d = 0.020$ and 0.052 m, for the Venoge and Chamberonne, respectively. Zero displacement height was situated below the roughness crests, $d \approx 0.80\overline{z_0}$.

Although the logarithmic law may well describe the velocity profile in the central depth region of the flow in the river Venoge, an overlap region where complete similarity occurs and where κ_e is universal and equal to 0.41 does not exist. In the case of the Chamberonne river, the equivalent von Karman constant was close to the universal value. It may be assumed that the differences observed between the two rivers may result from some roughness parameter possibly related to the distribution of the bed roughness elements.

Geometric parameters obtained for the river Venoge are in agreement with previous results by [27]. However, for the Chamberonne case, roughness height and zero-plane displacement height fall outside the expected range presented by Koll [27]. This may mainly be due to the difficulties in defining a geometric parameter which can reliably characterize the bed roughness for such low relative submergence.

Acknowledgements

The authors acknowledge the financial support of the Portuguese Science and Technology Foundation (BPD 21712/2005) and the Swiss National Science Foundation (2000-063818). M.J. Franca thanks W. Czernuszenko for fruitful discussions about the DAM methodology. Acknowledgements are due to John Beck for helping with the topographic data.

References

[1] Aberle J, Koll K. Double-averaged flow field over static armour layers. River Flow, vol. 1. London: Taylor & Francis; 2004. p. 225–33.
[2] Aberle J. Spatially averaged near-bed flow field over rough armour layers. River Flow, vol.1. London: Taylor & Francis; 2006. p. 153–62.
[3] Babaeyan-Koopaei K, Ervine DA, Carling PA, Cao Z. Velocity and turbulence measurements for two overbank flow events in river Severn. J Hydr Eng 2002;128(10):891–900.
[4] Baiamonte G, Giordano G, Ferro V. Advances on velocity profile and flow resistance law in gravel bed rivers. Excerpta 1995;9:41–89.
[5] Baiamonte G, Ferro V. The influence of roughness geometry and Shields parameter on flow resistance in gravel-bed channels. Earth Surf Proc Landforms 1997;22:759–72.
[6] Barenblatt GI. Scaling, self-similarity and intermediate asymptotics. Cambridge (UK): Cambridge University Press; 1996.
[7] Bathurst JC. Velocity profile in high-gradient, boulder-bed channels. Proc Int Conf Fluv Hydr 1988. Budapest.
[8] Bayazit M. Flow structure and sediment transport mechanics in steep channels. Euromech 156: Mech Sediment Transp 1982:197–206. Istanbul.
[9] Blanckaert K, Lemmin U. Means of noise reduction in acoustic turbulence measurements. J Hydr Res 2006;44:3–17.
[10] Buffin-Bélanger T, Roy AG. Effects of a pebble cluster on the turbulent structure of a depth-limited flow in a gravel-bed river. Geomorphology 1998;25:249–67.
[11] Buffin-Bélanger T, Roy AG. 1 min in the life of a river: selecting the optimal record length for the measurement of turbulence in fluvial boundary layers. Geomorphology 2005;68:77–94.
[12] Carravetta A, Della Morte R. Response of velocity to a sudden change of the bed roughness in sub critical open channel flow. River Flow, vol. 1. London: Taylor & Francis; 2004. p. 389–94.
[13] Clauser FH. The turbulent boundary layer. Adv Appl Mech 1956;4:1–51.
[14] Dittrich A, Koll K. Velocity field and resistance of flow over rough surface with large and small relative submergence. Int J Sediment Res 1997;12(3):21–33.
[15] Ferreira RML, Alves ECTL, Leal JGAB, Cardoso AH, editors. River Flow. London: Taylor & Francis; 2006.
[16] Ferro V, Baiamonte G. Flow velocity profiles in gravel-bed rivers. J Hydr Eng 1994;120(1):60–80.
[17] Franca MJ, Czernuszenko W. Equivalent velocity profile for turbulent flows over gravel riverbeds. River Flow, vol. 1. London: Taylor & Francis; 2006. p. 189–98.
[18] Franca MJ, Lemmin U. A field study of extremely rough, three-dimensional river flow. In: Proc of the 4th IAHR Int Symp on Envir Hydr. London: Taylor & Francis; 2004.
[19] Franca MJ, Lemmin U. Eliminating velocity aliasing in acoustic Doppler velocity profiler data. Meas Sci Technol 2006;17:313–22.
[20] Franca MJ, Lemmin U. Cross-section periodicity of turbulent gravel-bed river flows. In: Proc of the 4th River, Coastal, and Estuarine Morphodynamics: RCEM, vol. 1. London: Taylor & Francis; 2005. p. 203–10.
[21] Franca MJ. Flow dynamics over gravel riverbed. In: Proc of the XXXI IAHR Congress, Seoul; 2005.
[22] Hinze JO. Turbulence. New York: McGraw-Hill; 1975.
[23] Hurther D, Lemmin U, Blanckaert K. A field study of transport and mixing in a river, using an acoustic Doppler velocity profiler. River Flow, vol. 2. Lisse: Swets and Zeitlinger; 2002. p. 1205–212.
[24] Hurther D, Lemmin U. A correction method for turbulence measurements with a 3D acoustic Doppler velocity profiler. J Atmos Ocean Technol 2000;18:446–58.
[25] IATE/HYDRAM. Profil en long, profils en travers, et courbes de tarage des sections relevées. Rapport d'étude du Bassin Versant de la Venoge - HYDRAM/EPFL, Lausanne; 1996.
[26] Katul G, Wiberg P, Albertson J, Hornberger G. A mixing layer theory for flow resistance in shallow streams. Water Resour Res 2002;38(11):1250.
[27] Koll K. Parameterization of the vertical velocity profile in the wall region over rough surfaces. River Flow, vol. 1. London: Taylor & Francis; 2006. p. 163–72.
[28] Lopez F, Garcia MH. Mean flow and turbulence structure of open-channel flow through emergent vegetation. J Hydr Eng 2001;127(5):392–402.
[29] Marchand JP, Jarret RD, Jones LL. Velocity profile, surface slope, and bed material size for selected streams in Colorado. US Geol Survey – Open File Rep 1984:84–733.
[30] Monin AS, Yaglom AM. Statistical fluid mechanics: mechanics of turbulence, vol. 1. Cambridge (MA): MIT Press; 1971.
[31] Nelson JM, McLean SR, Wolfe SR. Mean flow and turbulence fields over two-dimensional bed forms. Water Resour Res 1993;29(12):3935–53.
[32] Nicholas AP. Computational fluid dynamics modelling of boundary roughness in gravel-bed rivers: an investigation of the effects of random variability in bed elevations. Earth Surf Proc Landforms 2001;26:345–62.
[33] Nikora V, Smart GM. Turbulence characteristics of New Zealand gravel-bed rivers. J Hydr Eng 1997;23(9):764–73.

[34] Nikora VI, Goring DG, McEwan IK, Griffiths G. Spatially averaged open-channel flow over rough bed. J Hydr Eng 2001;127(2):123–33.
[35] Nikora V, Koll K, McLean S, Dittrich A, Aberle J. Zero-plane displacement for rough-bed open-channel flows River Flow, vol. 1. Lisse: Swets and Zeitlinger; 2002. p. 83–91.
[36] Parker G, Garcia MH, editors. River, coastal, and estuarine morphodynamics: RCEM. London: Taylor & Francis; 2005.
[37] Pitlick J. Flow resistance under conditions of intense gravel transport. Water Resour Res 1992;28(3):891–903.
[38] Pokrajac D, Finnigan JJ, Manes C, McEwan I, Nikora V. On the definition of the shear velocity in rough bed open channel flows. River Flow, vol. 1. London: Taylor & Francis; 2006. p. 89–98.
[39] Polatel C, Muste M, Patel VC, Stoesser T, Rodi W. Double-averaged velocity profiles over large-scale roughness. In: Proc of the XXXI IAHR Congress, Seoul; 2005.
[40] Raupach MR, Shaw RH. Averaging procedures for flow within vegetation canopies. Boundary-Layer Meteorol 1982;22:79–90.
[41] Rolland T, Lemmin U. A two-component acoustic velocity profiler for use in turbulent open-channel flow. J Hydr Res 1997;35(4):545–61.
[42] Sanford TB, Lien RC. Turbulent properties in a homogeneous tidal bottom boundary layer. J Geophys Res 1999;104(C1):1245.
[43] Shen C, Lemmin U. Ultrasonic scattering in highly turbulent clear water flow. Ultrasonics 1997;35:57–64.
[44] Smart GM. Turbulent velocity profiles and boundary shear in gravel bed rivers. J Hydr Eng 1999;125(2):106–16.
[45] Smith JD, McLean SR. Spatially averaged flow over a wavy surface. J Geophys Res 1977;83(12):1735–46.
[46] Tritico HM, Hotchkiss RH. Unobstructed and obstructed turbulent flow in gravel bed rivers. J Hydr Eng 2005;131(8):635–45.
[47] Wolman MG. A method of sampling coarse river-bed material. Trans Amer Geoph Un 1954;35(6):951–6.
[48] Yang SQ, Tan SK, Lim SY. Velocity distribution and Dip-phenomenon in smooth uniform open channel flows. J Hydr Eng 2004;130(12):1179–86.